Mutations in *MAP3K1* Cause 46,XY Disorders of Sex Development and Implicate a Common Signal Transduction Pathway in Human Testis Determination

Alexander Pearlman,[1] Johnny Loke,[1] Cedric Le Caignec,[2,3] Stefan White,[4] Lisa Chin,[1] Andrew Friedman,[1] Nicholas Warr,[5] John Willan,[5] David Brauer,[1] Charles Farmer,[1] Eric Brooks,[1] Carole Oddoux,[1] Bridget Riley,[1] Shahin Shajahan,[1] Giovanna Camerino,[6] Tessa Homfray,[7] Andrew H. Crosby,[7] Jenny Couper,[8] Albert David,[2] Andy Greenfield,[5] Andrew Sinclair,[4] and Harry Ostrer[1,*]

Investigations of humans with disorders of sex development (DSDs) resulted in the discovery of many of the now-known mammalian sex-determining genes, including *SRY, RSPO1, SOX9*, *NR5A1*, *WT1*, *NR0B1*, and *WNT4*. Here, the locus for an autosomal sex-determining gene was mapped via linkage analysis in two families with 46,XY DSD to the long arm of chromosome 5 with a combined, multipoint parametric LOD score of 6.21. A splice-acceptor mutation (c.634-8T>A) in *MAP3K1* segregated with the phenotype in the first family and disrupted RNA splicing. Mutations were demonstrated in the second family (p.Gly616Arg) and in two of 11 sporadic cases (p.Leu189Pro, p.Leu189Arg)—18% prevalence in this cohort of sporadic cases. In cultured primary lymphoblastoid cells from family 1 and the two sporadic cases, these mutations altered the phosphorylation of the downstream targets, p38 and ERK1/2, and enhanced binding of RHOA to the MAP3K1 complex. *Map3k1* within the syntenic region was expressed in the embryonic mouse gonad prior to, and after, sex determination. Thus, mutations in *MAP3K1* that result in 46,XY DSD with partial or complete gonadal dysgenesis implicate this pathway in normal human sex determination.

Sex determination in mammals is genetically controlled, with the expression of *SRY* (MIM 480000) on the Y chromosome causing the undifferentiated gonad to develop as a testis.[1] In turn, hormones secreted by the testis cause the Wolffian ducts to differentiate as seminal vesicles, vas deferens, and epididymis, and the Müllerian ducts to regress. In the absence of a Y chromosome and expression of *SRY*, the undifferentiated gonad develops as an ovary, the Wolffian ducts regress, and the Müllerian ducts develop as Fallopian tubes, uterus, and the upper third of the vagina. If the process of gonadal development goes awry, disorders of sex development (DSDs) may result (46,XX DSD [MIM 400045], 46,XY DSD [MIM 400044]).[2] Previously, these were known as intersex disorders or as either male and female pseudohermaphroditism or true hermaphroditism.[3]

Among the genes that have been identified by studying individuals with 46,XX DSD are *SRY*[4] and *RSPO1* (MIM 609595).[5] Among those identified by studying individuals with 46,XY DSD are *SRY*,[6] *SOX9* (MIM 608160),[7] *NR5A1* (MIM 184757),[8] *WT1* (MIM 607102),[9,10] *NR0B1* (MIM 300473),[11] and *WNT4* (MIM 603490).[12] The phenotype of the affected individual, manifested by the degree of masculinization or feminization of the gonads and internal and/or external genitalia, is often determined by the specific genetic mutations and, presumably, modifier genes. Individuals may be completely masculinized or feminized or have ambiguous genitalia.

The heritable nature of 46,XY DSD was identified in the 1970s.[13–15] These studies anticipated sex-limited transmission of an autosomal-dominant or X-linked trait from parents with the nonpenetrant genotype (46,XX) to those with the penetrant genotype (46,XY), accounting for the obvious lack of reproductive fitness. Most of these families were lost to follow-up, but one was recruited in the 1990s for future linkage and positional cloning studies and is reported here.[15] Another family, with 11 affected individuals, was reported in 2003.[16] Here, we describe mutations in *MAP3K1* (MIM 600982) (also known as *MEKK1*) that are associated with both familial and sporadic cases of 46,XY DSD, including one in the index family. These studies add *MAP3K1* and the mitogen-activated protein kinase (MAPK) signaling pathway to the repertoire of genetic pathways that control normal human testis development and identify mutations in this gene as a prevalent cause of 46,XY DSD.

In 2003, we mapped a gene, which, when mutated, was likely to be causative of the phenotype in family 1, to the long arm of chromosome 5.[17] This family was from France, was of European descent, and included six women with 46,XY complete (IV-3 and IV-21 in Figure 1 and Table S1 [available online]) or partial (II-12, III-35, IV-2, and IV-27) gonadal dysgenesis. One of the women with partial gonadal dysgenesis (II-12) had clitoral hypertrophy and hirsutism. Three of the women had gonadal tumors

[1]Human Genetics Program, New York University School of Medicine, New York, NY 10016, USA; [2]CHU Nantes, Service de Génétique Medicale, 44093 Nantes, France; [3]INSERM, UMR915, l'Institut du thorax, 44007 Nantes, France; [4]Murdoch Children's Research Institute and Department of Paediatrics, University of Melbourne, Melbourne, VIC 3052, Australia; [5]MRC Mammalian Genetics Unit, Harwell, OX11 0RD, UK; [6]Dipartimento di Patologia Umana ed Ereditaria, Università di Pavia, 27100 Pavia, Italy; [7]Clinical Developmental Sciences, Saint George's Hospital Medical School, London SW17 0RE, UK; [8]Department of Diabetes & Endocrinology, Women's & Children's Hospital, Adelaide SA 5006, Australia
*Correspondence: harry.ostrer@nyumc.org
DOI 10.1016/j.ajhg.2010.11.003.

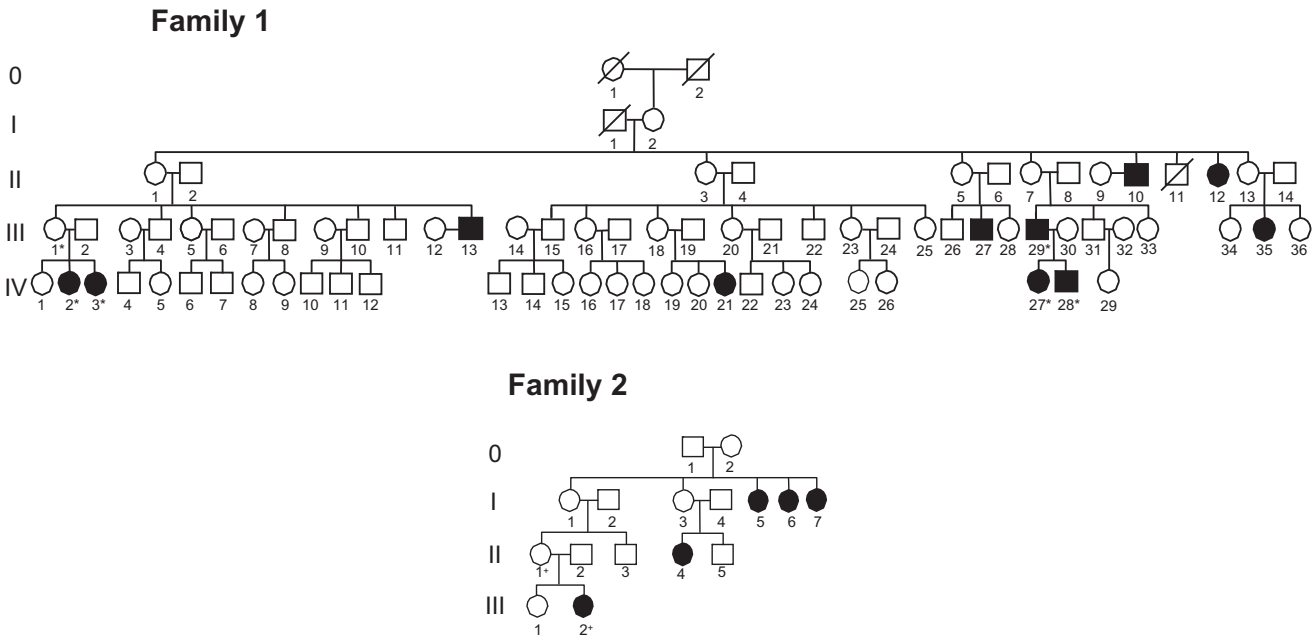

Figure 1. Pedigrees from Two Families of Interest Exhibiting Sex-Limited Autosomal-Dominant Mendelian Inheritance of 46,XY DSD
Shading indicates that the individual has 46,XY DSD or 46,XY complete gonadal dysgenesis. Circles indicate female sex of rearing, and squares indicate male sex of rearing. Asterisks (*) indicate individuals who were tested and found to have the c.IVS2-8T>A mutation. Plus signs (+) indicate individuals who were tested and found to have the p.Gly616Arg mutation. A strikethrough indicates a deceased individual.

(III-35, IV-2, and IV-3). Four men had genital abnormalities, including one with first-degree hypospadias with chordee (III-29) and three with perineal hypospadias (II-10, III-13, and IV-28). One of these individuals had micropenis and cryptorchidism (III-13). The man with first-degree hypospadias and chordee had normal fertility and fathered two children: one with perineal hypospadias and chordee (IV-28) and the other with 46,XY partial gonadal dysgenesis (IV-27). No extraurogenital abnormalities were observed in any individuals. Family 2 was from New Zealand and included five females with complete gonadal dysgenesis (II-5, II-6, II-7, III-4, and IV-2). This family was of Northern European origin and had a maximal LOD score of 1.14 at D5S2068 (see Table S2 for LOD scores and Table S3 for primer sequences). The combined LOD score for both families was 4.62 at D5S398; the multipoint LOD score was 6.21.

On the basis of linkage recombination breakpoints, the critical region between D5S1969 and D5S2028 encompassed 5 Mb of DNA and 34 candidate genes. Only two genes within this region, *Map3k1* (Figure 2) and *Mier3* (data not shown), demonstrated high levels of expression within 13.5 days postcoitum (dpc) in mouse gonads, and the expression was approximately equal in male and female gonads, as previously reported.[18] *Map3k1* expression was also observed throughout the mouse embryonic gonad at 11.5 dpc, the sex-determining stage of gonad development (Figure 2B).[19] Staining occurred within the testis cords at 13.5 dpc in a pattern indicative of Sertoli cell expression (Figure 2H).

Sequence analysis of *MIER3* (NM_152622.3) and *MAP3K1* (NM_005921.1) (Table S4) in affected individuals in the French family 1 identified only one previously unidentified heterozygous variant in the polypyrimidine track of the splice-acceptor site in intron 2 of *MAP3K1* (c.634-8T>A) that segregated with the phenotypes (Figure 3A). This variant of *MAP3K1* was not observed in 100 unrelated French individuals of European descent or in the 1000 Genomes Project. Given the proximity of this variant to the intron-exon boundary, a quantitative PCR assay was developed to test the efficiency or fidelity of mRNA splicing at this exon (Table S5). The level of expression for the normal and affected samples was not significantly different (Figure S1). However, variant cDNAs resulting in heteroduplex molecules were identified in samples from affected individuals by a second peak in the SYBR-green-based qPCR dissociation curves (Figure 3B). The splice products were analyzed by cloning and sequencing. The cloned cDNAs from the affected samples demonstrated both wild-type and aberrant splicing that resulted in the addition of six nucleotides into the RNA (c.633_634insAATCAG) and two amino acid residues (p.Val211_Val212insIleGln) into the protein in-frame at this site (Figure 3C). The ratio of the mutant to wild-type transcript was > 1 in the lymphophoblastoid cells of individuals carrying the mutation (Figure S1).

MAP3K1 was then sequenced in family 2 and in 11 sporadic cases. Mutations were identified in family 2 (c.1846G>A [p.Gly616Arg]) and in two unrelated sporadic cases of 46,XY complete gonadal dysgenesis (c.566T>C

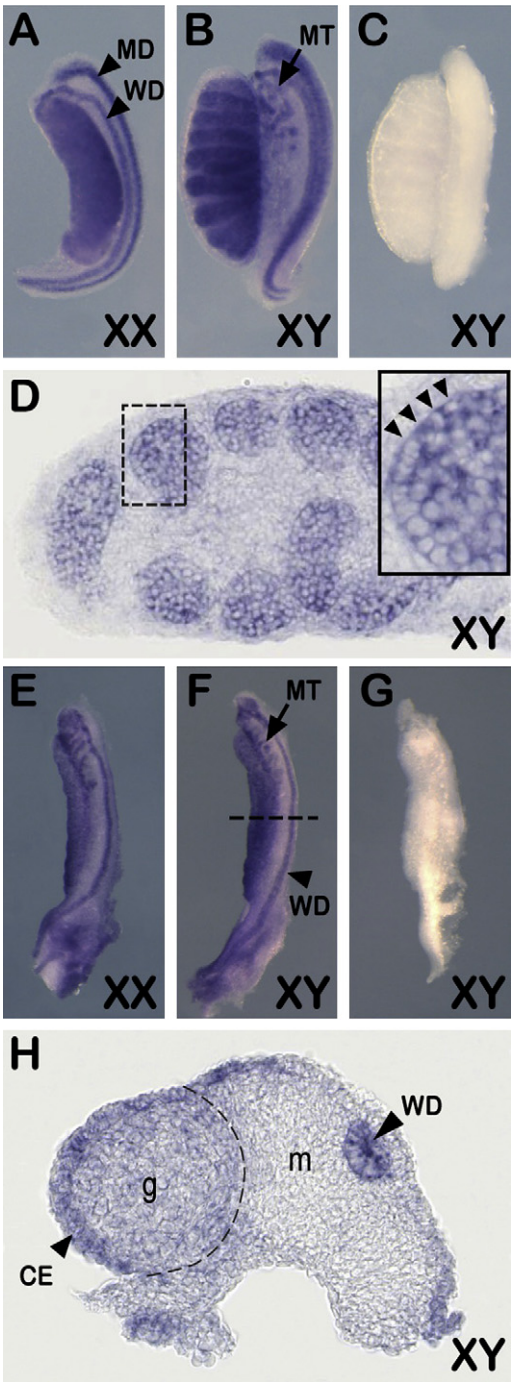

Figure 2. Whole-Mount In Situ Hybridization of Wild-Type Embryonic Gonads Reveals Strong Expression of *Map3k1* at the Sex-Determining Stage of Mouse Gonad Development

(A and B) Whole-mount staining of 13.5 dpc ovary (A) and testis (B). Expression is detected in the mesonephric tubules, Wolffian duct, and Müllerian duct of both sexes and in the testis cords in males.

(C) Negative control with sense RNA probe used.

(D) Longitudinal section through 13.5 dpc testis after *Map3k1* whole-mount in situ hybridization (WMISH). The staining is detected throughout the testis cords, and the smooth edge of this profile (arrowheads in inset showing high magnification image of cord in hatched box) indicates expression in Sertoli cells that abut the basement membrane.

(E and F) Whole-mount expression analysis of 11.5 dpc female (E) and male (F) gonads. The staining is prominent throughout the gonads of both sexes and is detected in the mesonephric tubules and associated Wolffian duct.

(G) Negative control with sense RNA probe used.

(H) Section of gonad shown in (B) (at level indicated by dashed line). Staining is detected throughout the gonad (g), in contrast to negligible staining in the adjacent mesonephric mesenchyme (m), but the signal is highest in the coelomic epithelium and subepithelial mesenchyme.

The dashed line in (G) indicates the boundary between gonad and mesonephros. Abbreviations are as follows: WD, Wolffian duct; MD, Müllerian duct; MT, mesonephric tubules; CE, coelomic epithelium; t, testis; m, mesonephros.

[p.Leu189Pro] and c.566T>G [p.Leu189Arg]) (Figure 3A). None of these variants was reported previously as a known SNP, nor were they observed in 100 unrelated, ethnically matched individuals tested specifically in our investigation or in the 1000 Genomes Project. No mutation was observed in nine other sporadic cases of 46,XY complete gonadal dysgenesis, suggesting a mutation prevalence of 18% in this cohort. The p.Leu189Pro and p.Leu189Arg mutations were reported by PolyPhen and SIFT[20] to be likely to interfere with function, whereas the heritable p.Gly616Arg mutation was not. Nonetheless, this mutation resulted in the substitution of a basic for a conserved neutral amino acid at this site. The p.Leu189Arg mutation was observed in the patient's mother, whereas the p.Leu189Pro mutation was not. The father of the patient with the p.Leu189Pro mutation was not available for analysis.

We then determined whether the mutations identified resulted in altered MAP3K1 function. Previously, it has been shown that MAP3K1 affects the MAP kinase cascade by regulating phosphorylation of the downstream targets p38 (MIM 600289), ERK1/2 (MIM 601795/MIM 176948), and JNK (MIM 605431).[21] The effects of three of the four *MAP3K1* mutations on phosphorylation of downstream targets were examined by quantitative immunoblot analysis after serum starvation for 24 hr and subsequent serum refeeding for an additional 1 hr in lymphoblastoid cells. (A cell line was not available for the p.Gly616Arg mutation.) Under these culture conditions, the phosphorylation of p38 in two out of three mutant cell lines was greater than wild-type, whereas levels of phospho-p38 in p.Leu189Pro were not altered (Figures 4A and 4B, Table S6—these increases were observed whether normalization was performed to histone or to total p38). Levels of phospho-ERK were increased in all the mutant cell lines in comparison to wild-type (Figures 4A and 4B, Table S6). Thus, we conclude that regulation of the MAPK signaling pathway is disrupted by the *MAP3K1* mutations reported here, causing increased activation in cultured lymphoblastoid cell lines.

To identify how these *MAP3K1* mutations might cause 46,XY DSD, we began by identifying their positions relative to the known protein-binding domains of MAP3K1. The intron splice-acceptor mutation in family 1 inserts two amino acids in the middle of a domain complementary to the interactive site of growth factor receptor-bound protein 2 (GRB2 [MIM 108355]),[22] and the point mutations at codon 189 occurred within the

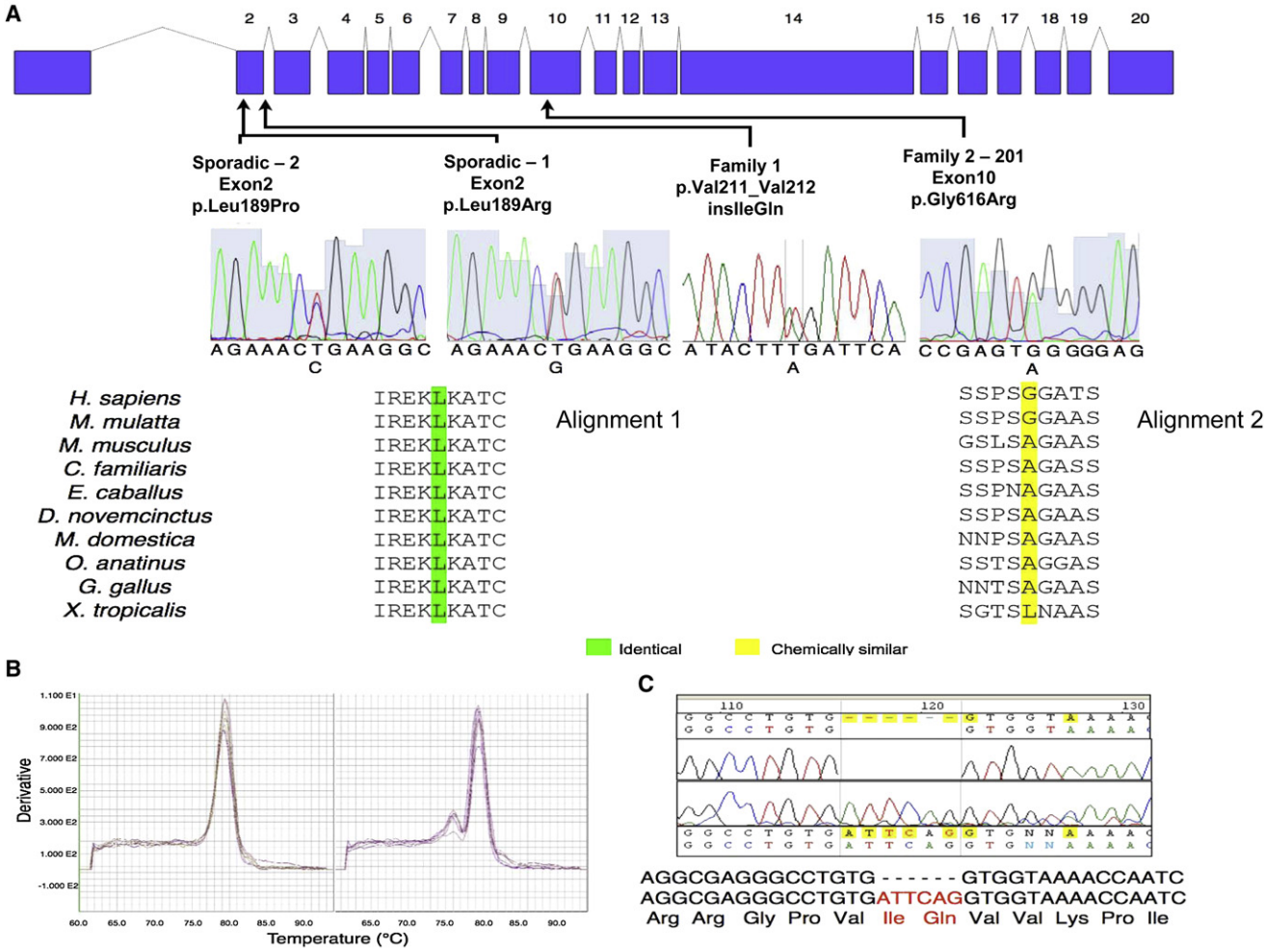

Figure 3. Mutations in *MAP3K1* in Patients with 46,XY DSD

(A) Schematic of *MAP3K1* structure and mutation locations. Sequencing chromatograms of four mutations identified an amino acid conservation taken from the UCSC Genome Browser. Alignment 1: invariant conservation of amino acids in ten species in the region of exon 2 where sporadic mutation 1 and sporadic mutation 2 lie. Alignment 2: the mutation in family 2 lies in a less highly conserved region.

(B) SYBR-green quantitative PCR dissociation curves. Control samples exhibited one form of cDNA with a single dissociation curve peak, whereas samples from family 1 exhibited heteroduplex and homoduplex cDNAs with two dissociation curve peaks indicating the presence of the mutant and wild-type forms.

(C) Chromatogram of *MAP3K1* cDNA demonstrating insertion of six nucleotides in-frame into the mutant mRNA (NM_005921.1:c.633_634insAATCAG) and two amino acid residues (p.Val211_Val212insIleGln) into the mutant protein.

phylogenetically conserved 27 amino acid region that comprises the focal adhesion kinase (FAK) binding site (MIM 600758).[23] Most significantly, all of these mutations and the codon 616 mutation occurred in the amino third of MAP3K1, a region that has been shown to interact with RHOA (MIM 165390).[24] That study showed that RHOA positively regulates MAP3K1 kinase activity by binding to its N-terminal third, in the region in which the mutations reported here have been identified.[24] To test whether *MAP3K1* mutations affected the binding of endogenous RHOA, we performed coimmunoprecipitation by immunoprecipitating mutant (c.634-8T>A) and wild-type complexes with anti-MAP3K1 and probing the immunoblot with anti-RHOA (Figure 4C). This experiment demonstrated that this mutation resulted in enhanced binding of RHOA in the mutant cell lines compared to wild-type. This increased binding could not be accounted for on the basis of unequal loading of MAP3K1-bearing complexes or on the basis of enhanced expression of RHOA in the mutant cell lines—as judged by immunoblot analysis (Figure 2S). In support of this finding, the converse immunoprecipitation experiments, with anti-RHOA, resulted in 2.1- to 2.8-fold increase in binding of MAP3K1 in three mutant cell lines compared to wild-type (p.Leu189Arg: $p = 0.0014$; p.Leu189Pro: $p = 4 \times 10^{-10}$; p.Val211_Val212insIleGln: $p = 0.0068$) (Figures 4D and 4E). Thus, enhanced binding of RHOA to MAP3K1 might account for the increased activation of MAPK signaling described earlier. The procedures were in accordance with the ethical standards of the New York University Langone Medical Center institutional review board (study

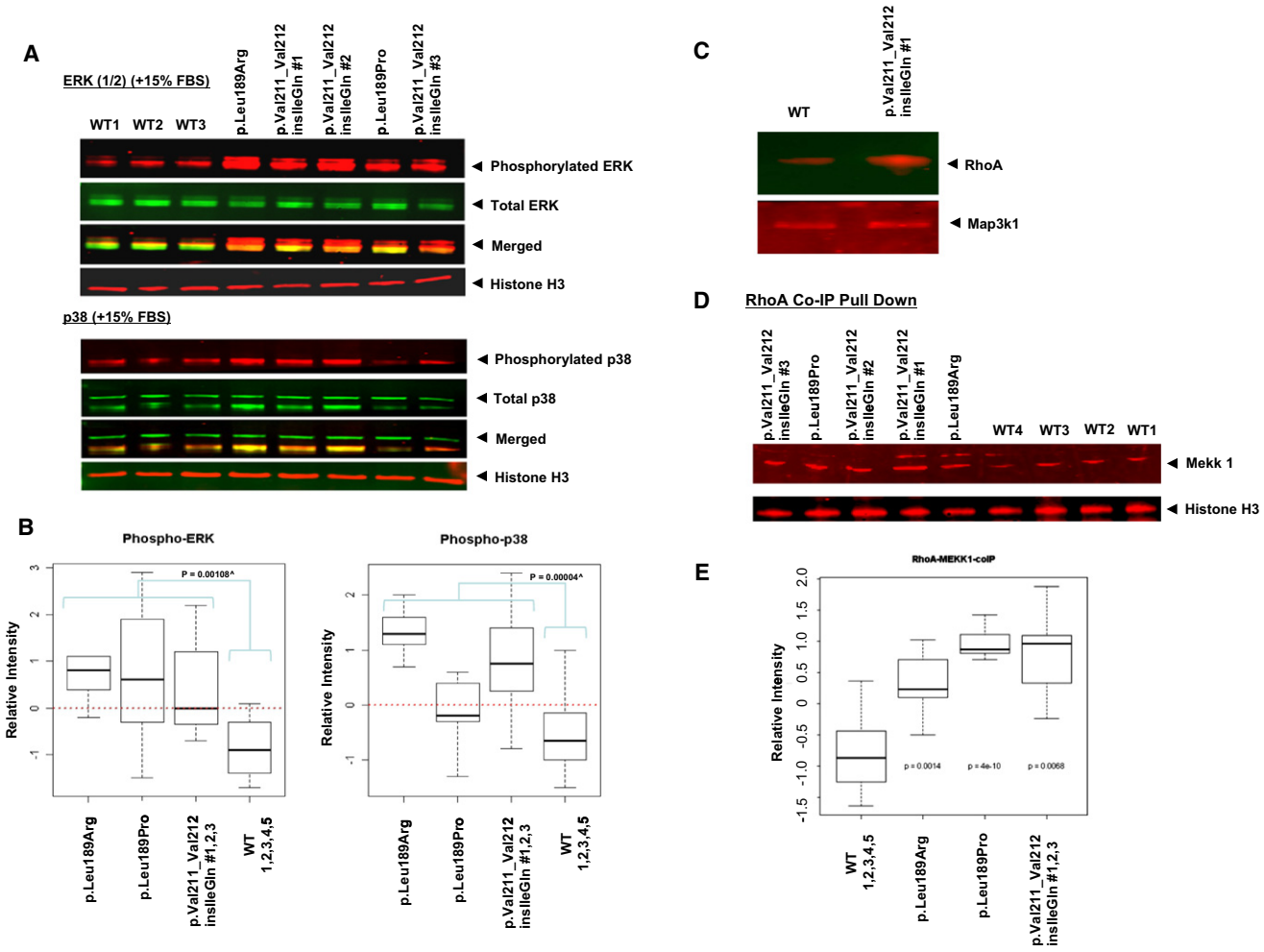

Figure 4. Effects of MAP3K1 Mutations on Phosphorylation of Downstream Targets and Binding of RHOA

(A) Dysregulation of MAPK signaling activity by *MAP3K1* mutations. Immunoblot analysis of cell lysates from human lymphoblastoid cell lines cultured in suspension in RPMI medium without serum supplemented with 1% penicillin and streptomycin for 24 hr, then refed serum for 1 hr. The blots were dual-hybridized overnight at 4°C with primary antibodies against phosphorylated and total p38 and ERK1/2 (both at 1:2000) and detected with the use of infrared dye-conjugated secondary antibodies (1:5000). The cell lines are designated as "WT" for wild-type or by the specific mutation and affected individual in family 1. Infrared absorbance detects phosphorylated signal at 680 nm (red) and total target activities at 800 nm (green). The histone H3 loading controls are also shown.

(B) Phosphorylated (phospho) p38 and ERK intensities normalized to histone H3 loading control intensity. The normalized intensities are indicated on the y axis, and the cell lines are indicated on the x axis. A box and whisker plot of p.Leu189Arg and p.Leu189Pro was represented by five measurements, whereas the p.Val211_Val212insIleGln and WT plots were represented by 15 and 25 measurements, respectively. The bottom and top whisker hash lines indicate the minimum and maximum values, the box length represents the interquartile range, and the dark horizontal line indicates the median of the data. The p values were determined by comparing the mutants to WT controls for each set of mutations with the use of the Student's t-test. Comparison of all mutant lines to all WT lines is denoted.

(C) Increased binding of RHOA to mutant MAP3K1. Proteins were immunoprecipitated with MAP3K1 antibody from lysates collected from mutant (p.Val211_Val212insIleGln) and wild-type cell lines and were probed on immunoblots with the RHOA . Upper panel: Mutant (p.Val211_Val212insIleGln) and wild-type cells were seeded in triplicates of 3 million cells. Triplicates were pooled and immunoprecipitated for each cell line. RHOA binding to MAP3K1 complexes in the wild-type (lane 1) was enhanced by the presence of the p.Val211_Val212insIleGln mutation in *MAP3K1* (lane 2). Lower panel: Equal loading of MAP3K1 complexes in each lane.

(D) Increased binding of mutant MAP3K1 to RHOA detected by immunoprecipitation. Mutant (p.Val211_Val212insIleGln, p.Leu189Pro, and p.Leu189Arg) and two wild-type cell line lysates were pooled from three independent experiments, totaling ~9 million cells per experiment, and pulled down (immunoprecipitated) with the use of anti-RHOA, then probed for MAP3K1 on immunoblots and normalized to the histone bands. Upper panel: MAP3K1 binding was enhanced by the presence of the p.Val211_Val212insIleGln, p.Leu189Arg, and p.Leu189Pro mutations in MAP3K1. Lower panel: Histone loading control of RHOA complexes in each lane.

(E) MAP3K1 intensities normalized to loading control intensity. The normalized intensities are indicated on the y axis, and the five cell lines are indicated on the x axis. A box and whisker plot of p.Leu189Arg and p.Leu189Pro was represented by five measurements, whereas the p.Val211_Val212insIleGln and WT plots were represented by 15 and 25 measurements, respectively. The p values were determined by comparing the mutants to WT controls for each mutation set with the use of the Student's t-test. Comparison of all mutant lines to all WT lines is denoted.

no. 10417), and proper informed consent was obtained. All mice were bred under standard conditions of care and used under licensed approval from the UK Home Office (PPL 30/2381).

An earlier study used linkage analysis and positional cloning in a family with 46,XX DSD and palmoplantar keratosis to identify *RSPO1* as the mutated, disease-associated gene.[5] The current study employed a similar approach to identify mutations in *MAP3K1* in families with 46,XY DSD and subsequently in sporadic cases with this phenotype. These in-frame mutations provide a basis for the autosomal-dominant, sex-limited inheritance. The phenotypic variation among affected members of family 1 might be explained by the individual differences in aberrant splicing in the developing gonad and, potentially, modifier loci. In mice with a spontaneously occurring loss-of-function, 8 exon deletion of *Map3k1* on a BALB/cGa background, the only reported phenotype was open eyelids at birth.[25] No genital abnormalities, skewing of the sex ratio, or infertility were reported in that study. However, unlike C57BL/6J, BALB/cGa is not a background known for its sensitivity to disruptions in testis development.

One other gene in the MAP kinase pathway has an established role in sex determination. Recently, some of us (A.G., N.W., and H.O.) identified the recessive boygirl (*byg*) mutation, which, when homozygous on the C57BL/6J background, resulted in embryos with XY gonadal sex reversal.[26] The *byg* mutation, an A-to-T transversion in *Map3k4* leading to a premature stop codon, caused a growth deficit in 11 dpc XY *byg/byg* gonads and a failure to support mesonephric cell migration, both early cellular processes normally associated with testis development. On some genetic backgrounds, XY mice merely heterozygous for a loss-of-function allele of *Map3k4* developed as viable females. Homozygous mutant 11.5 dpc XY gonads demonstrated a dramatic reduction in *Sox9* and *Sry* at the transcript and protein levels, accounting for the defect in Sertoli cell differentiation.

Here, we describe an unexpected activation of MAPK targets in human lymphoblastoid cells from the sex-reversing *MAP3K1* mutations. Given that loss of MAP3K4, and therefore a presumed deficit in MAPK signaling, causes XY sex reversal in mice, an apparent tension arises between observations in the two species. How might this be resolved? Members of the MAP kinase gene family could mediate the balance between the male and female sex-determining pathways by affecting the activities of the testis-promoting *SOX9* and *FGF9* (MIM 600921) and ovarian-promoting *WNT4* and *CTNNB1* (β-catenin) (MIM 116806) (reviewed in [27]). It is worth noting that such explanations do not require sexually dimorphic expression of MAPK signaling components during gonadogenesis because transcription of *SOX9*, *FGF9*, and *WNT4* is already sexually dimorphic. Previously, it has been shown that the transcriptional activity of SOX9 in chondrocytes is regulated by the MAP3K1 binding partner, RHOA,[28–30] and that the increase in SOX9 levels in chondrocytes induced by FGF2 (MIM 134920) is mediated via the MAP kinase pathway.[31] Axin (MIM 603816), a member of the MAPK complex and an inhibitor of the WNT signaling pathway, interacts with β-catenin to reduce its quantity.[32,33] Stabilization of β-catenin in the XY gonad causes male-to-female sex reversal, in part by reducing SOX9 expression.[34] Thus, the 46,XY DSD that is associated with mutations in MAP3K1 may be caused by decreased SOX9 activity, increased β-catenin activity, or both. Sorting through these possibilities and others will require further investigation, as will determining whether the functional consequences of specific MAP3K1 mutations in lymphoblastoid cell lines are similar to those in the embryonic gonad. Indeed, disruption to (loss of) one part of the MAPK signaling network is consistent with consequential activation of other components elsewhere.

In summary, we have identified mutations in *MAP3K1* that cause downstream alterations in the MAP kinase signaling pathway in two familial and two sporadic cases of 46,XY DSD. Mutations in this gene, as well as in *SRY*, *NR5A1*, and *DHH* (MIM 605423), should be routinely tested in individuals with 46,XY DSD.[2]

Supplemental Data

Supplemental Data include two figures and six tables and can be found with this article online at http://www.cell.com/AJHG/.

Acknowledgments

This study was supported in part by the US National Institutes of Health, the Medical Research Council of the United Kingdom, and the National Health and Medical Research Council of Australia.

Received: September 24, 2010
Revised: November 2, 2010
Accepted: November 9, 2010
Published online: December 2, 2010

Web Resources

The URLs for data presented herein are as follows:

1000 Genomes Project, http://www.1000genomes.org
Online Mendelian Inheritance in Man (OMIM), http://www.ncbi.nlm.nih.gov/Omim/
Polyphen, http://genetics.bwh.harvard.edu/pph/

References

1. Jost, A., Vigier, B., Prépin, J., and Perchellet, J.P. (1973). Studies on sex differentiation in mammals. Recent Prog. Horm. Res. *29*, 1–41.
2. Ostrer, H. (2008). 46,XY Disorder of sex development and 46,XY complete gonadal dysgenesis. In GeneReviews at GeneTests: Medical Genetics Information Resource. Roberta A. Pagon, ed. (Seattle: University of Washington. http://www.ncbi.nlm.nih.gov/bookshelf/br.fcgi?book=gene&part=gonad-dys-46xy.
3. Lee, P.A., Houk, C.P., Ahmed, S.F., and Hughes, I.A.; International Consensus Conference on Intersex organized by the

Lawson Wilkins Pediatric Endocrine Society and the European Society for Paediatric Endocrinology. (2006). Consensus statement on management of intersex disorders. Pediatrics *118*, e488–e500.
4. Sinclair, A.H., Berta, P., Palmer, M.S., Hawkins, J.R., Griffiths, B.L., Smith, M.J., Foster, J.W., Frischauf, A.M., Lovell-Badge, R., and Goodfellow, P.N. (1990). A gene from the human sex-determining region encodes a protein with homology to a conserved DNA-binding motif. Nature *346*, 240–244.
5. Parma, P., Radi, O., Vidal, V., Chaboissier, M.C., Dellambra, E., Valentini, S., Guerra, L., Schedl, A., and Camerino, G. (2006). R-spondin1 is essential in sex determination, skin differentiation and malignancy. Nat. Genet. *38*, 1304–1309.
6. Berta, P., Hawkins, J.R., Sinclair, A.H., Taylor, A., Griffiths, B.L., Goodfellow, P.N., and Fellous, M. (1990). Genetic evidence equating SRY and the testis-determining factor. Nature *348*, 448–450.
7. Foster, J.W., Dominguez-Steglich, M.A., Guioli, S., Kwok, C., Weller, P.A., Stevanović, M., Weissenbach, J., Mansour, S., Young, I.D., Goodfellow, P.N., et al. (1994). Campomelic dysplasia and autosomal sex reversal caused by mutations in an SRY-related gene. Nature *372*, 525–530.
8. Achermann, J.C., Ito, M., Ito, M., Hindmarsh, P.C., and Jameson, J.L. (1999). A mutation in the gene encoding steroidogenic factor-1 causes XY sex reversal and adrenal failure in humans. Nat. Genet. *22*, 125–126.
9. Hastie, N.D. (1992). Dominant negative mutations in the Wilms tumour (WT1) gene cause Denys-Drash syndrome—proof that a tumour-suppressor gene plays a crucial role in normal genitourinary development. Hum. Mol. Genet. *1*, 293–295.
10. Barbaux, S., Niaudet, P., Gubler, M.C., Grünfeld, J.P., Jaubert, F., Kuttenn, F., Fékété, C.N., Souleyreau-Therville, N., Thibaud, E., Fellous, M., and McElreavey, K. (1997). Donor splice-site mutations in WT1 are responsible for Frasier syndrome. Nat. Genet. *17*, 467–470.
11. Bardoni, B., Zanaria, E., Guioli, S., Floridia, G., Worley, K.C., Tonini, G., Ferrante, E., Chiumello, G., McCabe, E.R.B., Fraccaro, M., et al. (1994). A dosage sensitive locus at chromosome Xp21 is involved in male to female sex reversal. Nat. Genet. *7*, 497–501.
12. Jordan, B.K., Mohammed, M., Ching, S.T., Délot, E., Chen, X.N., Dewing, P., Swain, A., Rao, P.N., Elejalde, B.R., and Vilain, E. (2001). Up-regulation of WNT-4 signaling and dosage-sensitive sex reversal in humans. Am. J. Hum. Genet. *68*, 1102–1109.
13. Boczkowski, K. (1973). Abnormal sex determination and differentiation in man. Obstet. Gynecol. *41*, 310–314.
14. German, J., Simpson, J.L., Chaganti, R.S., Summitt, R.L., Reid, L.B., and Merkatz, I.R. (1978). Genetically determined sex-reversal in 46,XY humans. Science *202*, 53–56.
15. Espiner, E.A., Veale, A.M., Sands, V.E., and Fitzgerald, P.H. (1970). Familial syndrome of streak gonads and normal male karyotype in five phenotypic females. N. Engl. J. Med. *283*, 6–11.
16. Le Caignec, C., Baron, S., McElreavey, K., Joubert, M., Rival, J.M., Mechinaud, F., and David, A. (2003). 46,XY gonadal dysgenesis: evidence for autosomal dominant transmission in a large kindred. Am. J. Med. Genet. A. *116A*, 37–43.
17. Jawaheer, D., Juo, S.-H.H., Le Caignec, C., David, A., Petit, C., Gregersen, P., Dowbak, S., Damle, A., McElreavey, K., and Ostrer, H. (2003). Mapping a gene for 46,XY gonadal dysgenesis by linkage analysis. Clin. Genet. *63*, 530–535.
18. Beverdam, A., and Koopman, P. (2006). Expression profiling of purified mouse gonadal somatic cells during the critical time window of sex determination reveals novel candidate genes for human sexual dysgenesis syndromes. Hum. Mol. Genet. *15*, 417–431.
19. Karl, J., and Capel, B. (1998). Sertoli cells of the mouse testis originate from the coelomic epithelium. Dev. Biol. *203*, 323–333.
20. Ng, P.C., and Henikoff, S. (2003). SIFT: Predicting amino acid changes that affect protein function. Nucleic Acids Res. *31*, 3812–3814.
21. Cuevas, B.D., Abell, A.N., and Johnson, G.L. (2007). Role of mitogen-activated protein kinase kinase kinases in signal integration. Oncogene *26*, 3159–3171.
22. Nishida, M., Nagata, K., Hachimori, Y., Horiuchi, M., Ogura, K., Mandiyan, V., Schlessinger, J., and Inagaki, F. (2001). Novel recognition mode between Vav and Grb2 SH3 domains. EMBO J. *20*, 2995–3007.
23. Yujiri, T., Nawata, R., Takahashi, T., Sato, Y., Tanizawa, Y., Kitamura, T., and Oka, Y. (2003). MEK kinase 1 interacts with focal adhesion kinase and regulates insulin receptor substrate-1 expression. J. Biol. Chem. *278*, 3846–3851.
24. Gallagher, E.D., Gutowski, S., Sternweis, P.C., and Cobb, M.H. (2004). RhoA binds to the amino terminus of MEKK1 and regulates its kinase activity. J. Biol. Chem. *279*, 1872–1877.
25. Juriloff, D.M., Harris, M.J., and Mah, D.G. (2005). The open-eyelid mutation, lidgap-Gates, is an eight-exon deletion in the mouse Map3k1 gene. Genomics *85*, 139–142.
26. Bogani, D., Siggers, P., Brixey, R., Warr, N., Beddow, S., Edwards, J., Williams, D., Wilhelm, D., Koopman, P., Flavell, R.A., et al. (2009). Loss of mitogen-activated protein kinase kinase kinase 4 (MAP3K4) reveals a requirement for MAPK signalling in mouse sex determination. PLoS Biol. *7*, e1000196.
27. Cool, J., and Capel, B. (2009). Mixed signals: development of the testis. Semin. Reprod. Med. *27*, 5–13.
28. Tew, S.R., and Hardingham, T.E. (2006). Regulation of SOX9 mRNA in human articular chondrocytes involving p38 MAPK activation and mRNA stabilization. J. Biol. Chem. *281*, 39471–39479.
29. Woods, A., Wang, G., and Beier, F. (2005). RhoA/ROCK signaling regulates Sox9 expression and actin organization during chondrogenesis. J. Biol. Chem. *280*, 11626–11634.
30. Kumar, D., and Lassar, A.B. (2009). The transcriptional activity of Sox9 in chondrocytes is regulated by RhoA signaling and actin polymerization. Mol. Cell. Biol. *29*, 4262–4273.
31. Murakami, S., Kan, M., McKeehan, W.L., and de Crombrugghe, B. (2000). Up-regulation of the chondrogenic Sox9 gene by fibroblast growth factors is mediated by the mitogen-activated protein kinase pathway. Proc. Natl. Acad. Sci. USA *97*, 1113–1118.
32. Nakamura, T., Hamada, F., Ishidate, T., Anai, K., Kawahara, K., Toyoshima, K., and Akiyama, T. (1998). Axin, an inhibitor of the Wnt signalling pathway, interacts with beta-catenin, GSK-3beta and APC and reduces the beta-catenin level. Genes Cells *3*, 395–403.
33. Sue Ng, S., Mahmoudi, T., Li, V.S., Hatzis, P., Boersema, P.J., Mohammed, S., Heck, A.J., and Clevers, H. (2010). MAP3K1 functionally interacts with Axin1 in the canonical Wnt signalling pathway. Biol. Chem. *391*, 171–180.
34. Maatouk, D.M., DiNapoli, L., Alvers, A., Parker, K.L., Taketo, M.M., and Capel, B. (2008). Stabilization of beta-catenin in XY gonads causes male-to-female sex-reversal. Hum. Mol. Genet. *17*, 2949–2955.